Dissociation kinetics of hydrogen-passivated P_b defects at the (111)Si/SiO_2 interface

A. Stesmans
Department of Physics, University of Leuven, 3001 Leuven, Belgium
(Received 5 May 1999; revised manuscript received 24 August 1999)

An electron-spin-resonance study has been carried out, both isothermally and isochronically, of the recovery under vacuum annealing from the hydrogen passivated state (symbolized as HP_b) of paramagnetic P_b centers ($Si_3{\equiv}Si^{\bullet}$) at the (111)Si/SiO_2 interface. Previous work had reported simple exponential decay of $[P_bH]$ vs time, taken as key evidence for the process obeying the first-order rate equation $d[P_bH]/dt=-k_d[P_bH]$, where $k_d=k_{do}\exp(-E_d/kT)$ and E_d the single-valued activation energy. This inference, however, suffered from inadequate data. In contrast, experimental upgrading reveals manifest nonsimple exponential decay, which, within the simple thermal model, reveals the existence of a distinct spread σ_{E_d} in E_d. Incorporation of Gaussian spread in E_d leads to a consistent generalized simple thermal model, that matches physical insight. The broad range of data enabled unbiased determination of the physical parameters involved, giving $E_d=2.83\pm0.02$ eV, $\sigma_{E_d}=0.08\pm0.03$ eV, and attempt frequency $k_{do}=(1.6\pm0.5)\times10^{13}\,s^{-1}$, close to the Si-H waging mode frequency, which provides a clue to the atomic dissociation mechanism. The spread σ_{E_d} results from the interfacial stress-induced variations in P_b defect morphology. The body of data is found incompatible with second-order kinetics, thus exposing P_bH dissociation as an individual process. Combination with the previous generalized thermal model for P_b passivation with H_2 culminates in a consistent unified picture of the P_b-hydrogen interaction kinetics.

I. INTRODUCTION

It was recognized early on that the interface of thermally grown Si/SiO_2, the basic ingredient of current integrated circuit technology, suffers from the occurrence of electrically active centers.[1] Later, it was realized that hydrogen plays a prominent role in this matter as chemical reaction with hydrogen turned out to be an efficient way of inactivation, at least for some types of defects.[1–5] Hydrogen is always found present in Si/SiO_2 entities because of its universal presence during fabrication, explaining the inadvertent passivation in initial devices.

The subject is encountered in numerous studies (see, e.g., Refs. 2–12). Yet, only few works have aimed at inferring the specific trap-hydrogen interaction kinetics. Main techniques used include electrical capacitance-voltage (CV) measurements,[13,14] positron annihilation spectroscopy[15,16] (PAS), and electron-spin resonance (ESR),[17–21] where the former two appear to have been restricted to passivation and dissociation, respectively. Due to their inherent lack of atomic discriminative power, CV and PAS have appeared little decisive in model assessment, despite the impressive sensitivity of a technique such as CV. As known, there exist various types of interface traps.[22,23]

Though only few ESR works have addressed this matter, defect-type specific ESR is the technique of choice when the traps are paramagnetic, the so-called P_b-type defects—the generic ESR name for the class of paramagnetic coordination point defects[10,24–26] inherently generated at the interface as a result of mismatch.[27] Their appearance depends on the crystallographic interface orientation.[9,10] At the (111)Si/SiO_2 interface, the only type generally observed is specifically termed P_b. It was identified as trivalent interfacial Si, denoted $Si_3{\equiv}Si^{\bullet}$, where the dot symbolizes an unpaired electron in a dangling $sp^3{}_{\langle111\rangle}$-like orbital. They were shown to be electrically detrimental interface traps (see, e.g., Refs. 9 and 28). The (100)Si/SiO_2 structure exhibits two prominent types, termed P_{b0} and P_{b1}. For standard oxidation (800–950 °C), an areal density $[P_b]{\equiv}N_i{\sim}5\times10^{12}\,cm^{-2}$ [$\sim$0.6% of the atomic sites in a (111)Si plane] of defect sites (inactivated or not) is inherently incorporated.[27,29] All three P_b variants were shown to be trivalent Si centers, where the consensus is[30,31] that P_{b0} is the equivalent of P_b, but now residing at (imperfections of) a macroscopic (100)-oriented Si/SiO_2 interface. P_{b1} is hinted[32] to be a distorted defected interfacial Si dimer. For this important class of Si dangling-bond centers, electrical inactivation is generally pictured as chemical saturation of the failing bond by hydrogen, symbolized as SiH formation.[5,9,15] So far, however, there exists no direct experimental proof of this, which, in a reductionist attitude, is often readily forgotten.

II. P_b MOLECULAR HYDROGEN INTERACTION

A. Initial canonical picture

Some preliminary atomic insight on P_b hydrogen bonding was provided by initial ESR work,[10,24,25,33] some in combination with an electrical technique. In pioneering ESR work,[17,18] Brower was the first to fully quantify the hydrogen interaction kinetics of P_b's with *molecular* H_2. His model, henceforth called the simple thermal (ST) scheme, was soon accepted as definitive upon disclosure. It concerns a least-complications scheme, the red wire being that the key interactions are simply rate limited by the availability of ''reactive'' sites, i.e., $[P_b]$ and $[P_bH]$ for passivation and dissociation, respectively. The P_b passivation in *molecular* H_2 and dissociation in vacuum (studied in the temperature ranges $T=230-260$ and 500–590 °C, respectively) is modeled by the simple chemical reactions

TABLE I. Results within the generalized simple thermal (GST) model for thermal dissociation kinetics of P_bH entities at the interface of thermal (111)Si/SiO_2 (dry; $T_{OX}\sim 970\,^{\circ}C$). Previous results on passivation in H_2 are also included.

Reference	E_d (eV)	σ_{E_d} (eV)	k_{d0} ($10^{13}\,s^{-1}$)
	Dissociation		
This work	2.83 ± 0.02[a]	0.08 ± 0.03	1.6 ± 0.5
Ref. 18	2.56 ± 0.06[b]	0	~0.12
	Passivation		
	E_f (eV)	σ_{E_f} (eV)	k_{f0} ($10^{-8}\,cm^{-3}\,s^{-1}$)
Ref. 20	1.51 ± 0.04[c]	0.06 ± 0.004	9.8 $(+8/-5)$
Ref. 17	1.66 ± 0.06[b]	0	194 $(+200/-100)$

[a]GST model [see Eq. (5)].
[b]ST model; inadequate $[P_b]$ monitoring; dry oxide (1 atm O_2, 750–850 °C).
[c]GST model; dry oxide (1 atm O_2; 870 °C).

$$Si_3{\equiv}Si^{\bullet}+H_2\rightarrow Si_3{\equiv}SiH+H, \tag{1}$$

$$Si_3{\equiv}SiH\rightarrow Si_3{\equiv}Si^{\bullet}+H, \tag{2}$$

leading to the respective first-order differential rate equations $d[P_b]/dt=-k_f[H_2][P_b]$ and $d[P_b]/dt=k_d(N_0-[P_b])$, with solutions

$$[P_b]/N_0=\exp(-k_f[H_2]t), \tag{3}$$

$$[P_b]/N_0=1-\exp(-k_dt), \tag{4}$$

where the rate constants are given by the Arrhenius equations $k_f=k_{f0}\exp(-E_f/kT)$ and $k_d=k_{d0}\exp(-E_d/kT)$. Here, N_o is the initial density of P_b and HP_b entities (maximum number of recoverable ESR-active P_b centers), respectively, $[H_2]$ is the volume concentration of H_2 at the interface, and k is Boltzmann's constant. The inferred parameters were $E_f=1.66\pm0.06$ eV, $E_d=2.56\pm0.06$ eV, and preexponential factors $k_{f0}=1.94(+2/-1)\times10^{-6}\,cm^3/s$, $k_{d0}\approx1.2\times10^{12}\,s^{-1}$ (cf. Table I).

Regarding passivation, basic ingredients of the ST model include: (i) H_2 is physically absorbed into the SiO_2 layer and diffuses molecularly among the accessible interstices of the SiO_2 network, including the reaction site at the P_b center; (ii) rather than diffusion, the passivation is limited by direct P_b-H_2 reaction at the P_b reaction site; (iii) there is no preliminary cracking of H_2 molecules at internal sites in the SiO_2 on their way towards the interface; (iv) for both the passivation and dissociation steps, *single-valued* activation energies (E_f and E_d) are presumed.

B. Other work

The ST model enjoyed theoretical support[34] from semiempirical spin-unrestricted molecular-orbital calculations. Though without consideration of particular dissociation pathways, the values $E_f=1.32$ eV and $E_d=2.7$ eV were reported, in fair agreement with Brower's data[17,18] (1.66 and 2.56 eV, respectively). Of much interest are the results[35] based on the favored density-functional theory (DFT) addressing the Si-H bond placed in bulk Si. The work reports an energy $\sim$3.6 eV (the Si-H binding energy) needed for removing a neutral H^0 to free space (a position ''far'' away from the dangling bond), while a value $\sim$2.6 eV is found for a H^0 dissociating into a bulk Si site remote from the dangling bond (DB).

A recent ESR study[19] of P_bH dissociation applying isochronal ($2h$) annealing, *when interpreted within* the ST model, largely affirmed Brower's results.[18] However, the interpretation was carried out *assuming* first-order kinetics, whereby an appropriate value for k_{d0}, was *postulated*—it could not be inferred independently. The intertwined effect of E_d and k_{d0} in Eq. (4), in conjunction with the limited data extend, resulted in equally ''good'' fits for correlated variation of E_d and k_{d0} over unacceptably large ranges of 2.4–2.9 eV and 10^{11}–$10^{14}\,s^{-1}$—of little decisive power indeed. Likewise, PAS studies,[15] *assuming* first-order kinetics and $k_{d0}\sim1\times10^{13}\,s^{-1}$, reported the value $E_d=3.0\pm0.3$ eV for the release of H from interfacial (111)Si/SiO_2 regions. It should be noted, though, that the association in PAS with P_b-H dissociation is less direct than it is for ESR analysis, where the fingerprint of the P_b defect is monitored directly.

Finally, we add that the dissociation and passivation in H_2 of P_b-type defects has also been studied in (100)Si/SiO_2 by ESR and PAS. With respect to *dissociation*, X-band ESR work,[19] postulating $k_{d0}=2\times10^{13}\,s^{-1}$, reported $E_d=2.86\pm0.04$ and 2.91 ± 0.03 for P_{b0} and P_{b1}, respectively. On the other hand, *assuming* $k_{d0}=1\times10^{13}\,s^{-1}$, PAS experiments[16] found $E_d=2.60\pm0.06$ (corresponding to $E_d=2.65$ for $k_{d0}=2\times10^{13}\,s^{-1}$) for the global breakup of interfacial Si-H bonds, exposing some discrepancy. For PAS, however, it is unclear whether both types of defects are detected with equal sensitivity. An extensive (isothermal) ESR study[21] on *passivation* in H_2 reported the mean values $E_f=1.51\pm0.04$ and 1.57 ± 0.04 eV for P_{b0} and P_{b1}, respectively, while revealing for both defects the existence of a spread $\sigma_{E_f}=0.15\pm0.03$.

C. Revisiting P_b-hydrogen passivation kinetics

There are various reasons to readdress the ST model for P_b passivation kinetics in H_2. As noted before,[20] a first major one is the alleviation of a previous[17,18] inadvertent flaw in ESR experimenting regarding the correct monitoring of the P_b defect density, implying that the previous model inference was based on inadequate data. Likely, as a result of this, the previously inferred k_{d0} may appear unrealistically low (*vide infra*).

Second, there is the recent ESR reanalysis[20] of *passivation* kinetics of P_b in molecular hydrogen, demonstrating the failure of the ST model to account for the experimental data: Using isothermal annealing, the existence was demonstrated of a (previously unnoticed) intrinsic spread σ_{E_f} in E_f ascribed to nonidentical physical environments (strain) of the individual P_b's. Incorporation of this spread in the ST model led to a consistent general ST scheme, with the results shown in Table I; $k_{f0}[H_2]$ represents an attempt frequency, which, in contrast with the previous result,[17] now complies with underlying physical insight. It is then conceivable to expect a correlated analogous spread in the activation energy E_d for P_b-H dissociation.

Third, the available data set requires improvement and extension to an enlarged $[P_b]$ span (as expressed initially[18]) to enable unambiguous extraction of E_d and k_{d0} indepen-

dently. It would allow decisive model assessment. Finally, the total density of prevailing P_b sites, previously[17,18] merely left as a fitting parameter, has since been experimentally ascertained.[27,29]

The present work aims to thoroughly verify the ST model for dissociation in vacuum,[36] and if applicable, to determine E_d and k_{d0} independently. This is realized through providing broad data ranges with combination of both isothermal and isochronal annealing, extension to thermally enhanced P_b systems, and improved ESR spectroscopy, including reliable N_0 determination. The results will be seen to expose the existence of a spread in the activation energy for dissociation. When properly included, the amended ST model is found to describe all data consistently. In combination with the previous consolidated passivation scheme, it results in a solid global picture of the P_b-hydrogen interaction. Comparison with theory leads to interesting conclusions about the atomic pathway for P_bH dissociation.

III. EXPERIMENTAL DETAILS

A. Sample preparation

Slices of 2×9 mm^2 main face, appropriate for ESR, were cut from 2-in-diam commercial float-zone (111)Si wafers ($>100\ \Omega$ cm, *p*-type, two side polished) of thickness ~ 70 μm. Their 9-mm edge was a $\langle 110\rangle$ direction. After standard wet chemical cleaning, multiple samples (each comprising ~ 10 slices) were submitted to various thermal steps in a high-vacuum laboratory facility. The key part is a double wall high-purity silica tube inserting into a conventional mobile electronically stabilized (T stability better than 0.5 °C) tubular furnace with a 5.0-cm open bore, as described elsewhere.[27]

Temperature and its uniformity were carefully calibrated at the sample position using *S*-type (Pt: 13% Rh) thermocouples calibrated against the Pt thermometer standard. The accuracy reached on absolute T is $\leqslant 0.3$ °C, with a uniformity over the sample space better than 0.5 °C (radial gradient $\leqslant 0.2$ °C/cm). In the quartz insert, the sample slices were positioned in slits cut in a high-purity *U*-shaped quartz holder within an area $\leqslant 2$ cm^2. All equipment used for sample manipulation and cleaning was constructed from polytetrafluoroethylene.

The first thermal step implied oxidation at ~ 970 °C (1.1 atm dry O_2; 99.9995%; oxide thickness $d_{ox}\sim 42$ nm), terminated by rapid cooling to room temperature (RT) in O_2. This was standardly followed by a $\sim$40-min treatment in H_2 (1.1 atm; 99.9999%) at 405 °C in order to passivate all P_b's, as affirmed by ESR. This then establishes the starting condition for the dissociation study. A depassivation step was initiated by centering the furnace, preset at the desired T, over the diffusion pumped ($\leqslant 4\times 10^{-7}$ Torr) silica tube. The process was stopped by abruptly offsetting the furnace, thus allowing the samples to cool to RT in vacuum. Samples were annealed for appropriate times and desired temperatures in the range 480–970 °C, either isochronically or isothermally. The isochronal mode implied two types of investigations: In a first one, a freshly oxidized and subsequently fully passivated sample was used for each isochronal (62 min) vacuum annealing step—henceforth referred to as the fresh oxide samples set. In a second type, physically only two specimen were used. Upon oxidation, each was submitted to a post oxidation anneal (POA) in vacuum at 968 or $\sim$1000 °C for 1 h, in order to increase the P_b density through the creation mechanism[29] (*vide infra*). These are referred to as POA samples. These were then repeatedly submitted to alternately isochronal annealing and exhaustive repassivation (resetting initial conditions). The dissociation results of both procedures are found to coincide: While reassuring, it shows there is no need to use a freshly oxidized sample each time. As an interesting aspect, the one-sample procedure allows thorough verification of the thermal stability of the P_b system. After the initial high-vacuum forming anneal (968 °C, 1 h), which, through the parallel action of creation and dissociation mechanisms, results in a maximum number of paramagnetic P_b's, a first ESR diagnosis found N_0, the maximum density of recoverable defects as detected by ESR. If assuming, as likely, that H is the sole P_b passivation agent, N_0 will also represent the total number of P_b sites present. The completion of the extended dissociation study ended with a final exhaustive dissociation step at $\sim$968 °C (1 h). As compared to the initial starting condition, the observation then of an unchanged ESR spectrum and identical N_0 assured nothing irreversible had happened over the numerous thermal dissociation steps, in agreement with previous results.

To limit uncertainties, dissociation experiments should ideally be carried out by applying rectangular time-temperature vacuum anneal profiles. Clearly, the outlined procedure unavoidably deviates from ideality due to heating up and cooling transient effects. These need particular attention as the samples, kept in vacuum, can only thermally equilibrate with the furnace by heat exchange via thermal irradiation. Calibration of the transient steps show that upon insertion in the furnace it takes about 7–8 min for the inner evacuated silica tube to reach equilibrium, without noticeable overshoot. The sharp initial drop in T upon offsetting the furnace ($\geqslant 2$ °C/s), by contrast, makes the end effect error negligible. The transient effects have been corrected for. All thermal steps were halted by cooling to RT in unaltered ambient [semiexponential cooling process with cooling rate constant of $\sim$390 and 200 s in vacuum and gas ambient ($\sim$1.1 atm), respectively].

B. ESR spectrometry; P_b density determination

Conventional absorption mode ESR ($\sim$20.6 GHz) observations were made at 4.3 K, with the modulation amplitude ($\sim$0.25 G) of the applied magnetic field **B** and microwave power levels $P_\mu(<0.3$ nW) restricted to linear-response levels. The P_b spectra were always taken with $\mathbf{B}\|$ interface normal within 3°, assuring optimal sensitivity.[37]

Spin densities were determined by double numerical integration of the dP_μ/dB spectra relative to that of an isotropic Si:P spin standard signal recorded in one trace, always identically comounted with the (111)Si/SiO_2 sample bundle. Particular care was paid to the increasing ESR linewidth and line-shape alterations with increasing $[P_b]$ due to strengthening dipolar interaction,[38] which mandates appropriate adjustment of the B field integration window. This has been fixed at $\sim$54 G, centered at the P_b signal, appropriate for the highest $[P_b]$. The absolute spin-density accuracy is esti-

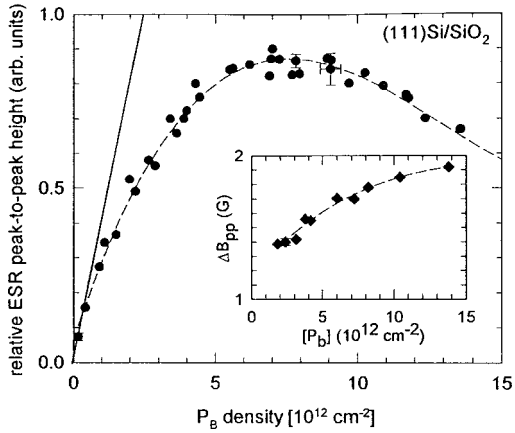

FIG. 1. Variation of the derivative-absorption ESR signal height $2V_D$ versus areal P_b density (determined via double numerical integration) in thermal (111)Si/SiO_2. The results include data both from as-oxidized samples and samples subsequently submitted to POA (968 or ~1000 °C). The P_b density is varied through (in pairs) anneal treatments in H_2 (405 °C) and vacuum at elevated temperatures. The solid line hints the ideal V_D-vs-$[P_b]$ behavior should no variation in ΔB_{pp} or line shape occur. The unveiled drastic deviation reflects the growing impact of dipolar interactions within the two-dimensional P_b spin bath with increasing density. The dashed curve is a least-squares cubic fit, guiding the eye. The inset shows the attendant variation in linewidth; the dashed curve guides the eye.

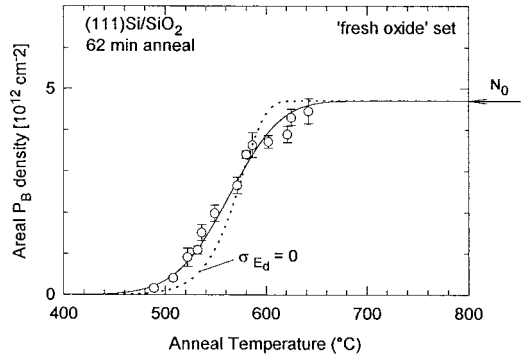

FIG. 2. Recovery of paramagnetic P_b defects (P_bH dissociation) by isochronal annealing in vacuum of the as-oxidized (111)Si/SiO_2 (''fresh oxide'') sample set for each data point, a freshly oxidized specimen is used, subsequently exhaustively passivated in H_2 (1.1 atm; 405 °C; ~40 min). The solid curve represents an optimized fit of the *generalized* simple thermal model [Eq. (5)], with the inferred parameters collected in Table I, revealing the existence of a spread $\sigma_{E_d}=0.08\pm0.03$ eV in activation energy. The dotted curve corresponds to an ''optimized'' fit for the ST model [Eq. (4)] using the same parameter values as listed in Table I, but with spread $\sigma_{E_d}=0$ (single-valued E_d), exposing the inadequacy of the description. The error bars represent the spread over typically 4–6 measurements.

mated at ~10%, while the relative accuracy may be better than 5%. Signals are averaged typically over ~10 traces; no digital filtering was applied.

In his work on the H-P_b interaction kinetics, Brower[17] clearly stated he used the peak-to-peak height $2V_D$ of the dP_μ/dB signal rather than orthodox double numerical integration (area under absorption curve). The main reason for this might have been signal-to-noise limitations with increasing P_b passivation level. But as previously noted,[20] that procedure is spectroscopically only justified if both the linewidth and shape remain unchanged—neither of which holds as later on manifestly exposed by analyzing (varying) dipolar interactions.[38] The failure of using V_D is dramatically exposed in Fig. 1, showing the relative variation of V_D-vs-areal P_b density. The inset shows the attendant variation in peak-to-peak linewidth ΔB_{pp} due to dipolar interaction among P_b's. Various items bear noting: First, should no change in line shape or width occur, a linear V_D-vs-$[P_b]$ relationship would ideally be expected, as previously supposed.[18] But obviously, as exemplified by the tangent (solid line) to the data for $[P_b]\rightarrow 0$, a linear relationship virtually holds nowhere—at best for $[P_b]\leqslant 0.5\times10^{12}\,\mathrm{cm}^{-2}$. Above this value, the deviation grows alarmingly. Second, even when restricting to the range below the natural P_b density N_i ($\sim5\times10^{12}\,\mathrm{cm}^{-2}$), the error in $[P_b]$ reading relative to the correctly determined one may amount to -2.5 when relying on a linear $[P_b]$-V_D relationship. Third, in the range $[P_b]=(4-12)\times10^{12}\,\mathrm{cm}^{-2}$, V_D varies little, with a maximal potential absolute error of a factor 3 if relying on V_D. Four, if disregarding saturability, Fig. 1 would indicate optimum ESR sensitivity for $[P_b]\sim(6-7)\times10^{12}\,\mathrm{cm}^{-2}$—about the N_i value. Hence, aiming to enhance ESR detectivity through enlarging $[P_b]$ above N_i would fail.

Previous work[17,18] also relied on the V_D method to cautiously verify the physical stability of the studied P_b entities—i.e., fixed P_b entity density N_0, either passivated by H or not—to ensure that the perceived H-P_b interaction effects were purely chemical in nature, implying only P_bH formation and dissociation. A positive conclusion was reached from a few POA experiments at 675–850 °C for ~0.5–1 h in vacuum on thermal (111)Si/SiO_2 (dry O_2, 1 atm), with no evident change in V_D. Ever since, this result was accepted as definite proof of the utmost stability of the P_b system (constant N_i) under thermal treatment. In sharp contrast, however, recent work[29] revealed that annealing in vacuum ($\leqslant5\times10^{-7}$ Torr), leads to significant irreversible creation (from ~640 °C onward) of extra P_b's in addition to the preexisting density N_i; e.g., at 850 °C, about $6\times10^{12}\,\mathrm{cm}^{-2}$ P_b's are created extra within minutes. Pertinently then, when hovering around in the range $[P_b]=(4-12)\times10^{12}\,\mathrm{cm}^{-2}$, it is clear at once from Fig. 1 how one may erroneously conclude from V_D an almost invariant signal strength.[39]

IV. EXPERIMENTAL RESULTS AND INTERPRETATION

Three sets of isochronal (~62 min) annealing data on P_bH depassivation in vacuum were measured. Figure 2 represents the fresh oxide set (each data point obtained on a freshly oxidized sample, subsequently exhaustively passivated in H_2), characterized by $N_0=(4.7\pm0.2)\times10^{12}\,\mathrm{cm}^{-2}=N_i$. The two sets of data shown in Fig. 3 correspond to the POA samples. To be noticed is the marked variation in N_0. As outlined, this is realized for the POA samples through the recently unveiled P_b creation mechanism,[29] implying that from ~640 °C onward, POA in vacuum leads to permanent irreversible creation of new P_b entities, in addition to the preexisting density N_i and indistinguishable from the latter.

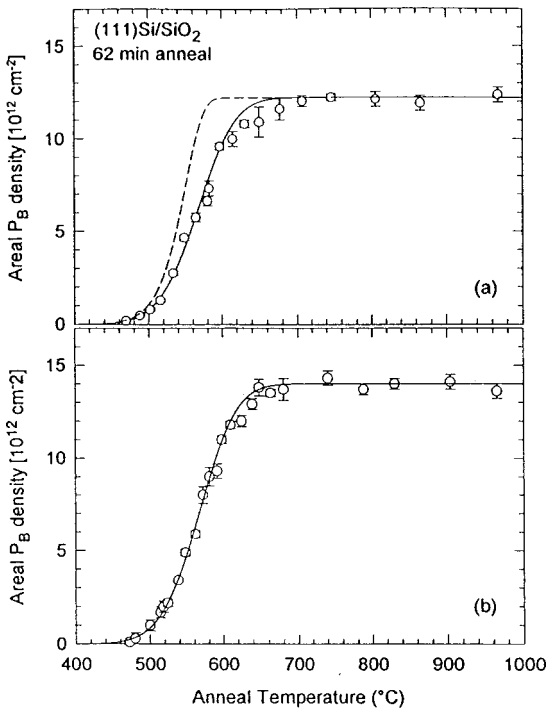

FIG. 3. Recovery of P_b defects by isochronal annealing in vacuum of (111)Si/SiO_2 structures initially ''degraded'' by POA at 968 °C (a) and ~1000 °C (b), resulting in $N_0=(12.2\pm0.2)$ and $(14\pm0.2)\times10^{12}\,cm^{-2}$, respectively. Solid curves are fits of the GST model [Eq. (5)] with the same parameter values (cf. Table I) as used in Fig. 2. The dashed curve in (a) is calculated from Eq. (4) (the ST model) using Brower's parameters (Ref. 18): $E_d=2.56$ eV; $k_{d0}=1.2\times10^{12}\,s^{-1}$.

The P_b creation (times ~1 h) increases monotonically with POA temperatures, the ultimately created P_b density being set by the POA treatment at highest T; no observable additional P_b's are created during subsequent POA at any lower T. While undoubtedly cumbersome for devices, one can take advantage of this creation mechanism in the present P_bH dissociation study. The applied POA (1 h; vacuum) at ~967 and 1000 °C creates P_b densities $N_C\sim7.3$ and $9.1\times10^{12}\,cm^{-2}$, resulting in $N_0=(12.2\pm0.2)$ [Fig. 3(a)] and $(14.0\pm0.2)\times10^{12}\,cm^{-2}$ [Fig. 3(b)], respectively.

One may wonder about the reliable determination of N_0 for the fresh oxide sample set. Clearly, one cannot apply T's above ~640 °C to map the reassuring N_0 plateau as done isochronically for the degraded samples (cf. Fig. 3), as this would alter N_0 due to the creation effect. (For the same reason, isochronal studies for the fresh oxide set must obviously also be restricted to the $T\leqslant640$ °C range; Fig. 2.) A first value of N_0 is provided by the as-oxidized state P_b density, measured as $N_0=(4.7\pm0.2)\times10^{12}\,cm^{-2}\sim N_i$ as expected.[19] It indicates that H contamination during oxidation in the used facility is insignificant. Yet, to enhance confidence, $[P_b](N_0)$ was also measured after prolonged exhaustive isothermal annealing in vacuum for ~29 h at 537 °C—a T well below the creation range—giving the same result. Thus, N_0 is not simply left as a fitting parameter.

According to the ST model, the data should check with the first-order kinetics Eq. (4). However, fitting this equation faces two major obstacles. First, with k_{d0} and E_d as fitting parameters to be extracted, no satisfactory fit can be attained.

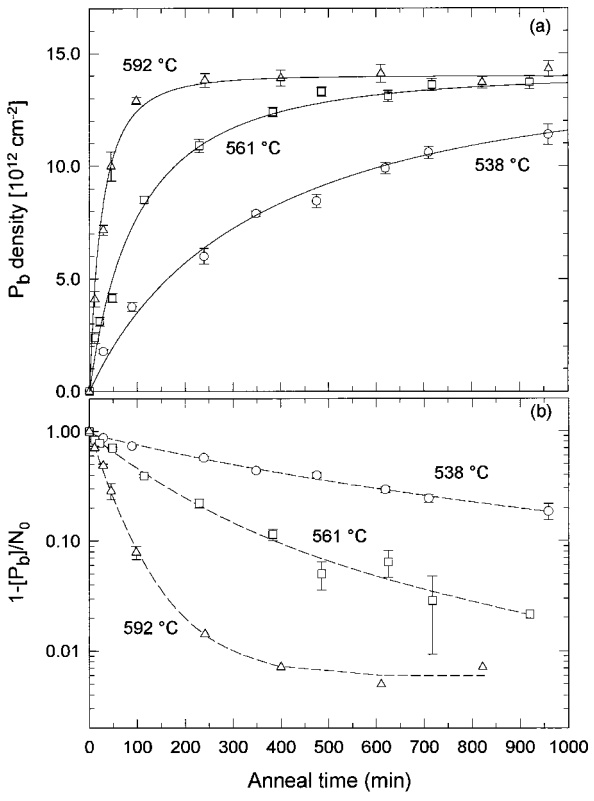

FIG. 4. (a) Isothermal recovery of P_b centers in the degraded (111)Si/SiO_2 sample of $N_0=14\times10^{12}\,cm^{-2}$. The curves represent a global fit of the GST model [Eq. (5)], giving the parameters collected in Table I. Within the ST model, the existence of a spread $\sigma_{E_d}\sim0.08$ eV in E_d is revealed. (b) Semilogarithmic replot as the fraction of P_bH centers $(=1-[P_b]/N_0)$ versus anneal time. The dashed curves are guides to the eye, exposing nonexponential decay.

The failure is strikingly exposed in Fig. 2 by the dotted curve, representing a ''best'' fit obtained with $E_d=2.92$ eV for a *postulated* value $k_{d0}=1.6\times10^{13}\,s^{-1}$. The major shortcoming is clear: the dissociation behavior as a function of T prescribed by Eq. (4) appears far too abrupt for the more stretched out data. The same conclusion applies for the fresh oxide set (Fig. 3). For comparison, also shown (dashed line) is the prescribed dissociation behavior [Eq. (4)] using previous parameter values[18] ($k_{d0}=1.2\times10^{12}\,s^{-1}$; $E_d=2.56$ eV), exposing the inadequacy of the ST scheme. Second, with respect to the aimed inference of k_{d0} and E_d, the fitting to the isochronal data is far from unique—not even with a much improved set of data as shown—due to the strong correlation of these parameters in Eq. (4). This was blatantly exposed in previous work.[19]

Clearly, improving reliability will require different practice. This is achieved by resorting to isothermal study. The results, obtained for $T=538$, 561, and 592 °C on the sample of $N_0\sim14.0\times10^{12}\,cm^{-2}$ are assembled in Fig. 4. According to Eq. (4) (the ST model), the data, when plotted as a logarithm of the fraction of P_bH centers $(=1-[P_b]/N_0)$ versus time t, should exhibit linear behavior. Such plot is shown in Fig. 4(b), from where, quite in contrast, there is little evidence for straight lines, exposing discrepancy. Here it should be recalled that in a similar semilogarithmic plot using the

relative P_b *signal heights* $(1-V_D/V_{D0})$ versus t, Brower[18] could fit his data with straight lines, which suggested true exponential decay of $[P_b]$ vs t. It was this apparent simple exponential decay that was taken as proof for the first-order kinetics [Eq. (4)] pertaining to the simple chemical reaction $P_b\mathrm{H}\rightarrow P_b+\mathrm{H}$. But, as outlined, this $[P_b]$ monitoring through V_D is unjustified. As strikingly exposed in Fig. 4(b), the P_bH decay is nonexponential,[40] thus apparently invalidating the main incentive for the model embraced by Eq. (4). [In support, it should be added that even in the initial work, monitoring V_D, the data in the semilogarithmic plot (cf. Fig. 6 in Ref. 18) are not convincingly arranged linearly; a curvature may clearly be perceived.] Rather, main observations in Fig. 4(b) are (i) as most prominent from the highest anneal temperature data, an initial steep drop in P_bH density over about the first hour of desorption and (ii) a gradual curving down with increasing t, without, however, much linear trend, except when exhaustive dissociation is reached.

One could then conclude the deduced P_bH dissociation model to be plainly incorrect. This, however, is not necessarily so, at least what concerns the underlaying basis [Eq. (2)]. As mentioned, the hint came from recent ESR-based reanalysis[20] of the passivation kinetics of P_b-type defects in Si/SiO_2. There, the existence of a spread $\sigma_{E_f}(\sim 0.06\,\mathrm{eV})$ in $E_f(\sim 1.51\,\mathrm{eV})$ was demonstrated. Inherently, a correlated spread σ_{E_d} in E_d may be expected.

There also seems to exist direct indication from the data for the existence of such spread in E_d. For one, there is the remarkable observation of the steep drop in $[P_b\mathrm{H}]$ over the first period of dissociation. In one opinion, this may indeed be reminiscent of nonuniformity within the P_b system as regards E_d, i.e., the existence of a spread: in terms of the isothermal data (Fig. 4), the fraction of P_bH centers possessing a lower E_d than average will accordingly dissociate more readily, thus accounting for the initial relatively steep drop in time. Those with larger E_d's account for the tailing. In turn, the isochronal data (Figs. 2 and 3) show the experimental dissociation to be pertinently more stretched out than predicted by the ST model [Eq. (4)], which may also be accounted for by a spread in E_d. It would provide a direct experimental evidence for the existence of such spread. This contrasts with previous work, where likely due to experimental scatter, no evidence for σ_{E_d} was concluded, although it was mentioned some spread could exist.[19] More evidence comes from a previous P_b ESR study[27] demonstrating that the interfacial P_b system exhibits a configurational distribution (larger for lower T_{ox}) correlated with interface stress. Facing the existence of interfacial strain, it may then appear surprising the spread in E_d has not been incorporated as a fact before.

Accordingly, the ST model is amended for the existence of spread in E_d, henceforth referred to as the generalized ST (GST) model. This is simply accomplished from Eq. (4), if assuming, as a first approach, a Gaussian distribution in E_d characterized by a standard deviation σ_{E_d}, leading to the generalized dissociation formula

$$[P_b]/N_0=1-\frac{1}{\sqrt{2\pi}\sigma_{E_d}}\int_0^{\infty} e^{[-(E_{di}-E_d)^2/2\sigma_{E_d}{}^2]} \times e^{[-tk_{d0}\exp(-E_{di}/\mathrm{kT})]}\,dE_{di}, \tag{5}$$

where E_d now represents the *mean* activation energy. Clearly, a payoff is that the much enhanced complexity of this model [Eq. (5)] hampers data interpretation; one can no longer resort to the simple fitting of straight lines, enabling straightforward extraction of E_d and k_{d0}. Instead, all data must be self-consistently fitted together. Though interpretatively more cumbersome, a successful fit is readily obtained, as illustrated by the solid lines in Fig. 4(a). The deduced parameters are listed in Table I, revealing a spread $\sigma_{E_d}=0.08\pm 0.02\,\mathrm{eV}$. An equally satisfactory fit (solid lines) is obtained for the isochronal data displayed in Figs. 2 and 3, for the *same* values of the parameters k_{d0}, E_d, and σ_{E_d} as given in Table I. When referring to expression (5), wherein N_0 appears just as a prefactor, it means that all isochronal data, when normalized, coincide. The success in fitting supports the underlying modified model.

One more remark on the accuracy of the deduced parameters may be useful. As outlined, isochronal data alone (Figs. 2 and 3) do not enable accurate unbiased determination of both E_d and k_{d0} independently. This is also true for the present enhanced sets of data, interpreted within the GST scheme, although the compatible k_{d0}-E_d ranges (inaccuracy windows) are drastically narrowed. The deduced value for $\sigma_{E_d}(=0.08\pm 0.03)$ is far more unique, the reason being that σ_{E_d} mainly ''accounts for'' the stretching out of the isochronal anneal curves. This highly unsatisfactory situation can only be remedied by invoking complementary isothermal analysis and varying both T and t over large ranges. The addition of various isothermal dissociation cycles adds more ''equations,'' leading to a faithful determination of all three parameters involved; it is the global fit over all data together that complies with scientific rigor. It is much significant that the isothermal approach was chosen in the initial work.[18]

V. DISCUSSION

A. GST model

A first comment concerns the inferred existence of the previously unrecognized spread σ_{E_d} in E_d. As hinted from previous ESR work, its physical origin is ascribed to variations in the local defect morphology over the P_b ensemble, affecting the Si:H bond strength via weak orbital rearrangements: over the various sites of these archetype interface defects, there exists[27] a stress-induced spread σ_h $(\sim 0.05-0.5\,\text{Å})$ in the mean distance of the apex Si atom to the plane formed by the three backbonded Si's. It seems natural that this will be reflected as a spread in E_d.

The existence of the spread in σ_{E_d} is manifested in other observations. First, as mentioned, recent reanalysis of the passivation kinetics[20] in H_2 of P_b (and[21] P_{b0}, P_{b1}) defects indicated the existence of spread σ_{E_f} in E_f. Obviously, if such spread exists in the activation energy for passivation, it will reverberate in the dissociation energy E_d. Second, perhaps most convincing, there is the long-known electrical fact that the P_b energy levels in the band gap exhibit a significant excessive distribution[9,10,33] (several tens of eV). Finally, in other work on defects in comparable circumstances, the existence of a spread in activation energy was recognized indeed.[41]

Next the derived value for k_{d0} is addressed. As outlined, the global fit of the GST model to all available data convincingly gives $k_{d0}=(1.6\pm0.5)\times10^{13}\,s^{-1}$, thus differing significantly from the previously inferred low value[18] of $\sim1.2\times10^{12}\,s^{-1}$. The latter may appear inconsistently low: Within the simple reaction-rate theory, the preexponential factor k_{d0} represents an attempt frequency, which for the present Si hydrogen interaction case should be accounted for by an appropriate Si-H vibrational mode. The k_{d0} value inferred here within the GST model is now found to be reassuringly close to the known low-frequency ($Si_3{\equiv}Si$-H) wagging mode[42] at 1.86×10^{13} Hz. It thus appears that with the GST scheme, fitting all available experimental data, a truly consistent *interpretative* model has been attained. The fact now that the inferred k_{d0} value is in compliance with a consolidated vibration frequency (wagging mode) of the Si-H bond strongly suggests that its underlaying basis also concerns the correct physical picture.

Another remark concerns the P_{b0} and P_{b1} defects at the technologically preferred (100)Si/SiO_2 interface. As a major result, the present study in conjunction with previous work[20] carried out along the same lines (proper ESR analysis, extended data ranges) has evidenced the existence of distinct spreads in both E_f and E_d for P_b. Interestingly, similar work[21] on passivation in H_2 for (100)Si/SiO_2 (1.1 atm O_2: 176 °C; $d_{ox}\sim2$ nm) has also revealed spreads $\sigma_{E_f}\sim0.15$ eV in E_f for both P_{b0} and P_{b1}. Hence, when carrying over from the P_b case, the activation energy for *dissociation* of P_{b0} and P_{b1} is also expected to exhibit noticeable spreads. This is the more so for P_{b0}, pictured as equivalent to P_b. Yet, the one ESR-based research[19] on this matter had to remain inconclusive, merely because of limited data. Among others, the existence of spreads in activation energies for passivation and dissociation has implications for technological interface defect control. For one, the existence of $\sigma_{E_f}(P_{b0},P_{b1})$ reduces the passivation efficiency of these defects in a typical H_2 ($\sim400\,°C;30'$) treatment. Also, the existence of σ_{E_f} and σ_{E_d} is particularly pertinent when facing reality implying that in an H_2 treatment, both processes, i.e., P_bH formation and dissociation, continuously operate simultaneously, albeit in much different efficiencies. This is unlike the standard analyses carried out so far, where, in an idealized approach, the influence of the reverse (much) less efficient step is considered negligible,[18,43] e.g., P_bH dissociation during an H_2 anneal. This matter will be dealt with elsewhere.

B. Si-H dissociation pathway

The measured value of $E_d(2.83\,\text{eV})$, and in particular $k_{d0}(\sim1.6\times10^{13}\,s^{-1})$, indicating that the low-frequency Si-H wagging mode controls thermal interfacial Si-H breaking—not the higher-frequency stretch mode[35,42] ($\sim6.8\times10^{13}$ Hz)—may provide a clue to the way H is physically detached. Within the context of recent DFT work[35] on the Si-H bond properties in Si, these data favor a dissociation pathway where, in an initial step, the wagging *neutral* H atom moves toward a Si-Si bond center site next to the DB, as depicted in Fig. 5. During this jump, the defected Si-H atom distance stays approximately constant (bond lengths Si-H, 1.48 Å; Si-Si, 0.235 Å). In a second step, with much reduced activation energy, the H atom can easily proceed its way to a position remote from the DB, possibly by trapping charge. Interstitial H will subsequently lower its energy, e.g., by H_2 molecule formation, perhaps eventually escaping molecularly into the open SiO_2 structure. This mechanism could thus suggest a significant role of carriers in interfacial Si-H dissociation. An effective $E_d\sim2.6$ eV was calculated. Importantly, initial H detachment from P_bH would thus occur via the Si side. The data disqualify a model where a H^0, with stretch-mode attempt frequency, would directly dissociate into the oxide (free-space-like environment). There are two more remarks. First, one may question whether the difference between the measured and calculated $E_d(2.83\pm0.02$ and 2.6 eV, respectively) is to be considered significant, or just scientifically satisfactory. Second, the sketched pathway is the favored one provided that the energy of H in a-SiO_2 is close to its energy in free space, as commonly accepted.[34]

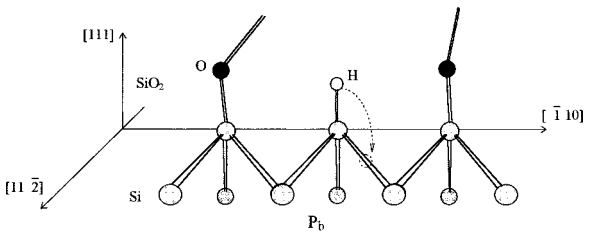

FIG. 5. Schematic illustration of H dissociation from P_bH. The path pictures H removal via the Si side, where in a first step (through the SiH wagging mode), H moves towards a neighboring Si-Si bond center site.

The role of the charge state was also addressed in previous molecular-orbital theoretical work.[34] With respect to the dissociation of P_bH, close values of the activation energy for hydrogen detachment were calculated for the neutral ($E_d=2.7$ eV) and positive (2.3 eV) charge state. However, the negative charge state would dissociate much easier, i.e., calculated $E_d\sim1.62$ eV. Conversely, passivation in H_2 under positive bias (P_b in negative charge state) is predicted to be much reduced—within the ST model, an anticipated reduction of 8 orders of magnitude in forward rate constant k_f. This still awaits experimental verification. We note that the calculated neutral case value ($E_d=2.7$ eV) is closest to the present value of 2.83 ± 0.02 eV. If the calculated difference between the neutral and positive charged case, i.e., 2.3 vs 2.7 eV, is deemed sufficiently reliable, this would also indicate the (first step in) P_b depassivation to occur predominantly in the *neutral* state.

C. Pathway for H_2 dissociation: Energy barriers

As noted previously,[8,11,18] the sequence of the elementary chemical reactions (1) and (2), describing P_b passivation and P_bH dissociation, constitutes a reaction mechanism for cracking of the H_2 molecule in SiO_2 (more correctly, in interstices at the Si/SiO_2 interface), the P_b acting as a catalyst. The apparent net activation energy is obtained as $E_t=E_f+E_d=4.34\pm0.06$ eV (cf. Table I)—remarkably close to the vacuum value $E_{H_2}^{vac}=4.52$ eV, even closer than the previously deduced ST value ~4.22. The GST model pictures H_2 crack-

ing as occurring at the very reactive site (including the P_b defect and its adjacent vacant site), that is, at the very interface region with no intermediate interactions (i.e., cracking and/or absorption at traps) of the diffusing H_2 in the bulk of the SiO_2 film. Then, if the measured value of E_t may indeed be taken as $E_{H_2}^{SiO_2}$, the activation energy for dissociation of the H_2 molecule in SiO_2, it is thus found that $E_{H_2}^{SiO_2}$ is slightly smaller than $E_{H_2}^{vac}$, as might be expected for dissociation in an SiO_2 network. While a difference may indeed be expected, it is also expected to be small.[18] One argument advanced is that SiO_2 is a rather tightly bound insulator (band gap $\sim$9 eV). Another argument is that the observed ESR high-frequency (hf) splitting of atomic H^0 in SiO_2 at low T is within 1% of the vacuum splitting.

A crucial point in this reasoning,[18] however, is the possible occurrence of intermediate energy barriers (to either the passivation or dissociation processes), i.e., unbalance between the derived E_f,E_d, and the energy differences between the initial and final constituents; if negligible, then the reverse passivation and dissociation reactions would proceed essentially spontaneously in the presence of atomic H. So, E_t must be considered as an upper limit to $E_{H_2}^{SiO_2}$:$E_{H_2}^{SiO_2} \leqslant E_t$. Should there exist a (weak) intermediate barrier to either process [Eqs. (1) and (2)], then $E_{H_2}^{SiO_2}$ will be reduced accordingly. We shall limit the discussion here as it has been addressed at length previously.[18] There, along a type of self-consistent reasoning, the key conclusion was E_t to be very close to $E_{H_2}^{SiO_2}$. The matter, however, is controversial:[44] in effect, a value $E_t - E_{H_2}^{SiO_2} \sim 0.1-0.2$ eV may apply. For one, some works,[13,23] though not quantifying, suggest the dominance of reverse dissociation ($P_b + H \rightarrow P_bH$) over the reverse passivation reaction ($P_bH + H \rightarrow P_b + H_2$), pointing to the existence of an activation energy for the latter. Obviously, clarification of this matter will require extensive studies in atomic H.

D. Other models

As discussed, the GST model provides a consistent physical picture that accounts for all data *en bloc*. Yet, a successful fit of all data available by parametrized equations, however satisfactory, does not necessarily imply that the underlying model represents physical reality. Here, in particular, it needs to be remarked that in comparison with the previous ST scheme, the consistent GST picture for P_b activation was reached for a major part through incorporation of the uncovered existence of the spread σ_{E_d} in E_d, that is, adding one more parameter. To this should be added, very pertinently, that a main basis—true single exponential decay of $[P_bH]$ vs t—underlying the previous conclusion[18] in favor of the ST model has dropped: a single set of $[P_bH]$-vs-t data does not provide direct unambiguous proof for first-order kinetics. So, scientific objectivity demands utmost care. In particular, models disavowing first-order kinetics might be considered, as a stretched decay may be reminiscent of higher-order kinetics.

1. Oxygen interstitial diffusion model

This model was perused in initial work.[18] It suggests itself since the activation energy for diffusion of bond-centered interstitial O in Si is characterized by[45] $E_a(O) = 2.54$ eV, close to the then inferred activation energy (2.56 ± 0.6 eV) for P_bH dissociation. According to this model, the rate limiting step for P_b recovery would be the diffusion of mobile interstitial O in Si towards P_b sites, where O would spontaneously react with the P_bH center, resulting in the formation of an OH radical that readily escapes from the P_b site. This O interstitial model was ruled out for various reasons, such as the inadequacy in accounting for the observed hydrogen isotopic effects and the O-P_b reactivity rate.[18,46] The present work provides one more reason, in fact, for not having had to consider it at all: the measured value $E_d = 2.83 \pm 0.02$ eV *vis-à-vis* $E_a(O) = 2.54$ eV would reject the model outright.

2. Second-order kinetics

As alluded to, the major indication for considering the possibility of non-first-order kinetics behavior came from the fact that the $[P_bH]$-vs-t data do not exhibit the simple exponential decay expected for first-order kinetics with a single-valued activation energy. In the isochronal mode, it appears reflected by the stretched out nature of the data, as shown in Fig. 2: The recovery of P_b's extends over too broad a temperature range than reconcilable with the single-valued E_d first-order ST description (dotted curve). In the GST model, this is accounted for by the incorporation of the spread σ_{E_d}($\sim$0.08 eV). However, both features may also be reminiscent of second-order kinetics (*vide infra*), which merits further attention.

Before entering this interpretative route, though, the basic question arises of how one may conceive the ''simple'' dissociation of P_bH entities, or more objectively, P_b reactivation, as a second-order process. Here it may prove useful recalling a well-known, somewhat related case for liberation of adsorbed species from a surface, i.e., the thermal detachment of absorbed atomic H at a pristine Si or metal surface.[47,48] Generally, this process involves, first, formation of molecular H_2 through thermal migration of atomic H over the surface (rate constant k_D'), which subsequently desorps *molecularly* (rate constant k_D). As the dimerization represents the rate limiting step (i.e., $k_D \gg k_D'$), the H-desorption process is described by a second-order rate equation $d[H(t)]/dt = -k_D'[H(t)]^2$, characterized by $E_a = 2.4$–2.8 eV. With this textbook example as a backdrop, one may pursue second-order scenarios for the P_b case. As basic guide in this may serve the reverse passivation reaction [Eq. (1)] in the presence of *atomic* H, admitted to proceed essentially spontaneously (*vide supra*); the formed molecular H_2 may then readily escape through the oxide into the ambient. Hence, along this guideline, one may speculate about possible means of how atomic H may be delivered to the P_bH sites. Obviously, we should primarily focus on inter- (P_b) defect interaction.

In a pushing first ansatz, one might envision a mechanism similar to the Si surface H-desorption case by simply adducing migration possibilities to P_bH's over the interface.[7] Where two P_bH centers come close, H_2 is released resulting in two unpassivated P_b's. (We refrain from any energetic

feasibility consideration of this process). Such picture, however, would likely strongly conflict with the utmost thermal stability of the P_b sites, i.e., strict preservation of their number and the marked reversibility in passivation and/or dissociation behavior. At least, there is so far no experimental evidence for migration at all. In a less extreme version, one could additionally speculate on the P_b defects predominantly occurring clustered, or in close pairs. However, we hasten to add that there is so far no evidence for a clustered distribution; instead, the ESR dipolar interaction data indicate random distribution over terraces.[38]

Second, one may speculate on the fact that even in nominally dry thermal oxide, a large quantity of H (in atomic form, after irradiation at 4 K) is generally detected[49] by ESR: $\sim 3\times 10^{12}\,\mathrm{cm}^{-2}$ in a 135-nm-thick oxide ($\sim$10 at. ppm volume concentration), a figure emphasized as being just a lower limit. This is well substantiated in a review,[50] indicating the presence of $\sim 10^{19}-10^{20}$ hydrogen species cm^{-3} as $\equiv$Si-OH and $\equiv$Si-H groups in steam- and O_2-grown oxides, respectively. It is confirmed by numerous experiments, the secondary ion mass spectroscopy[33] and nuclear reaction data[51] furthermore revealing a nonuniform distribution: there is substantial H pileup in the interface region. As to the P_bH dissociation then, one might hypothesize that the process is initiated by cracking off in the *direct* neighborhood of the P_bH an atomic H from some site(s) X pertaining to near-interfacial oxide or Si layers: the released atomic H would almost exclusively recombine with P_bH, so it could not diffuse to neighboring P_b sites to cause marring (re)passivation. The latter would result eventually in an intermediate (incomplete) dissociation level, quite in contrast with experimental observation. For the same reason, the X sites cannot be remotely distributed. We leave the precise nature of such sites unaddressed, although one might speculate about several. We just add that it cannot concern thermal release of atomic H from a *bulk* $O_3\equiv$Si-H defect (passivated E') because the strength[52] of this Si-H bond ($\sim$4 eV) prevents any significant H release in the pertinent T range 500–700 °C. Anyhow, such scenario would lead to second-order kinetics with rate equation $d[P_b\mathrm{H}]/dt=-k_D''[X][P_b\mathrm{H}]$, where we notice that the condition $[X]\geqslant[P_b\mathrm{H}]$ is required, i.e., $[X]\geqslant 5\times 10^{12}\,\mathrm{cm}^{-2}$, to enable the observed complete P_bH dissociation. The case $[X]\approx[P_b\mathrm{H}]$ would suggest during oxidation P_b and X to be incorporated as conjugated pairs.

To illustrate the second-order interpretation, we take as prototype the first process discussed, described by the rate equation

$$d[P_b\mathrm{H}]/dt=-k_d'[P_b\mathrm{H}]^2=k_d'(N_0-[P_b])^2, \qquad (6)$$

with solution

$$[P_b]=N_0-[1/N_0+k_d't]^{-1}, \qquad (7)$$

where $k_d'=k_{d0}'\exp(E_d'/\mathrm{kT})$. The fitting of this expression is illustrated for the isochronal data in Fig. 6, where arbitrarily, we have chosen to optimize the fit to the fresh oxide data set. And indeed, as exposed by the solid curve (fresh oxide set), a much satisfactory fit is obtained using $k_{d0}'=5.7\times 10^{-3}\,\mathrm{cm}^2\,\mathrm{s}^{-1}$ and $E_d'\sim 2.32$ eV, unlike the single-valued E_d ST model[53] [cf. dashed curve in Fig. 3(a)]. The stretched out trend for the transition region is seen to be well

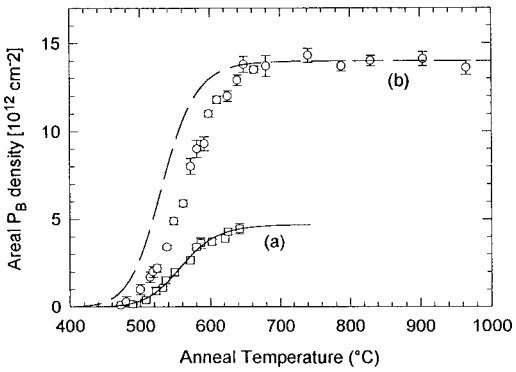

FIG. 6. Fit of second-order kinetics expression (7) to two sets of isochronal vacuum annealing results for P_b recovery. As optimized to the ''fresh oxide'' set [(a) solid curve; $N_0=N_i$], the fitting fails dramatically for the $N_0=14\times 10^{12}\,\mathrm{cm}^{-2}$ data [(b) dashed curve], thus rejecting second-order kinetics.

reproduced—an intrinsic property of the second-order-type kinetics. In effect, scientific objectivity forces us to state that the fitting of an *individual* set of isochronal dissociation data pertaining to one P_b bath of density N_0 does not enable discrimination between the GST model (first-order) or second-order kinetics. The deficiency of the latter becomes only obvious when extending to all data. As to the isochronal data, this is manifestly exposed in Fig. 6.: while the fitting of Eq. (7) to the $N_0=4.7\times 10^{12}\,\mathrm{cm}^{-2}$ data appears perfect, the fitting (dotted curve) of the $N_0=14\times 10^{12}\,\mathrm{cm}^{-2}$ results using the *same* E_d' and k_{d0}' fails disappointingly. The inadequacy is even more blatantly exposed by the isothermal data (not shown), where consistent fitting fails dramatically. Trying to remedy the situation here by also introducing a spread $\sigma_{E_d'}$ in E_d', similar to the GST case, makes things only worse. Hence, we conclude that the P_b recovery kinetics are at odds with second-order expression (7), which provides one more support for the validity of the GST model.

The failure of second-order kinetics fitting may after all not be surprising. As evidenced in the preceding section, the isochronal data of all three samples of distinctly different N_0, when normalized for N_0, fall on top of each other. Such conduct is discordant with the second-order expression (7): Unlike the first-order case, N_0 here does not just appear as a simple prefactor. It underlines the importance in this research of comparing samples of significantly different N_0.

VI. CONCLUDING REMARKS

Using K-band ESR, the thermal recovery kinetics of P_b's in standard thermal (111)Si/SiO_2 has been studied with particular attention to proper ESR spectroscopy and providing a sufficiently complete set of data, both isothermally and isochronically, so as to enable conclusive model verification and unambiguous parameter determination.

As basic experimental finding, the isothermal dissociation data $[P_b\mathrm{H}]$ vs time exhibit a manifest nonsimple exponential decay, while the isochronal annealing curves exhibit a stretched out nature, incompatible with simple exponential decay. These features reveal the existence of a spread $\sigma_{E_d}\sim 0.08$ eV in the activation energy for dissociation around the mean value $E_d=2.83\pm 0.02$ eV. The spread reflects the

interface stress-induced nonuniformity of the P_b defects. By incorporating this spread as a Gaussian distribution, the previous ST scheme for P_b recovery may be upgraded to a consistent model. The Si-H wagging vibration is inferred as the relevant attempt frequency for dissociation, reflecting the self-consistency of the underlying model. It favors the atomic path where H dissociates via the Si side, the first step implying a ''wagging'' jump of the bonded H atom into an adjacent Si-Si bond-center site, from where the H atom may subsequently escape after charge trapping.

The body of experimental data is incompatible with a homomolecular second-order kinetics scenario as, e.g., rate limiting the desorption of H from a passivated free Si surface. It affirms the P_b recovery as an *individual* thermal process. The dissociation of P_bH entities by interaction with atomic H (inverse passivation reaction) released nearby is not a feasible scenario for dissociation in vacuum.

Recent extensive work[20] on *passivation* kinetics of P_b in H_2 has also demonstrated the presence of a spread σ_{E_f} in E_f, the inclusion of which in the simple P_b-H_2 reaction limited passivation model led to a consistent picture. Also here, the inferred preexponential factor is found in compliance with underlying physics. Hence, when combined with the present results, a truly unified consistent picture of the P_b-hydrogen interaction kinetics is obtained, that matches physical insight. It is argued that the attained model also applies to the P_{b0} and P_{b1} defects in (100)Si/SiO_2. This may not appear surprising as recent progress has shown the key part of P_{b1}, like P_b, to be an interfacial dangling Si bond as well, albeit with dissimilar backbond configurations. The latter just accounts for some difference in the values of the pertinent physical quantities involved (e.g., E_f, σ_{E_f}).

[1] Y. C. Cheng, Prog. Surf. Sci. **8**, 181 (1977), and references therein.

[2] D. M. Brown and P. V. Gray, J. Electrochem. Soc. **115**, 760 (1968).

[3] S. R. Hofstein, Solid-State Electron. **10**, 657 (1967).

[4] P. L. Castro and B. E. Deal, J. Electrochem. Soc. **118**, 280 (1971).

[5] F. Montillo and P. Balk, J. Electrochem. Soc. **118**, 1463 (1971).

[6] D. L. Griscom, J. Appl. Phys. **58**, 2524 (1985).

[7] L. Do Thang and P. Balk, J. Electrochem. Soc. **135**, 1797 (1988).

[8] S. M. Meyers and P. M. Richards, J. Appl. Phys. **67**, 4064 (1990).

[9] R. Helms and E. Poindexter, Rep. Prog. Phys. **57**, 791 (1994), and references therein.

[10] E. H. Poindexter and P. J. Caplan, Prog. Surf. Sci. **14**, 201 (1983), and references therein.

[11] K. L. Brower and S. M. Meyers, Appl. Phys. Lett. **57**, 162 (1990).

[12] E. H. Poindexter, Z. Naturforsch., A: Phys. Sci. **50**, 653 (1995).

[13] M. L. Reed and J. D. Plummer, J. Appl. Phys. **63**, 5776 (1988).

[14] E. P. Burte, J. Appl. Phys. **64**, 5013 (1988).

[15] K. G. Lynn, B. Nielsen, and D. O. Welch, Can. J. Phys. **67**, 818 (1989).

[16] R. Khatri, P. Asoka-Kumar, B. Nielsen, L. O. Roellig, and K. G. Lynn, Appl. Phys. Lett. **65**, 330 (1994).

[17] K. L. Brower, Phys. Rev. B **38**, 9657 (1988).

[18] K. L. Brower, Phys. Rev. B **42**, 3444 (1990).

[19] J. H. Stathis, J. Appl. Phys. **77**, 6205 (1995); **78**, 5215 (1995).

[20] A. Stesmans, Appl. Phys. Lett. **68**, 2723 (1996).

[21] A. Stesmans, Appl. Phys. Lett. **68**, 2076 (1996).

[22] C.-T. Sah, J. Y.-C. Sun, and J. J.-T. Tsou, J. Appl. Phys. **55**, 1525 (1984); L. Trombetta, G. Gerardi, D. J. DiMaria, and E. Tierney, *ibid.* **64**, 2434 (1988).

[23] E. Cartier, J. H. Stathis, and D. A. Buchanan, Appl. Phys. Lett. **63**, 1510 (1993).

[24] Y. Nishi, Jpn. J. Appl. Phys. **10**, 52 (1971).

[25] E. H. Poindexter, P. Caplan, B. Deal, and R. Razouk, J. Appl. Phys. **52**, 879 (1981).

[26] For a review on Si/SiO_2 defect physics, see Semicond. Sci. Technol. **4**, 961 (1989).

[27] A. Stesmans, Phys. Rev. B **48**, 2418 (1993); Solid State Commun. **96**, 397 (1995).

[28] G. J. Gerardi, E. H. Poindexter, P. J. Caplan, and N. M. Johnson, Appl. Phys. Lett. **49**, 348 (1986).

[29] A. Stesmans and V. V. Afanas'ev, Phys. Rev. B **54**, R11 129 (1996).

[30] J. W. Gabrys, P. M. Lenahan, and W. Weber, Microelectron. Eng. **22**, 273 (1993).

[31] A. Stesmans and V. V. Afanas'ev, J. Appl. Phys. **83**, 2449 (1998).

[32] A. Stesmans, B. Nouwen, and V. V. Afanas'ev, Phys. Rev. B **58**, 15 801 (1998).

[33] N. M. Johnson, D. K. Biegelsen, and M. D. Moyer, J. Vac. Sci. Technol. **19**, 390 (1981).

[34] A. H. Edwards, Phys. Rev. B **44**, 1832 (1991).

[35] C. G. Van de Walle and R. B. Street, Phys. Rev. B **49**, 14 766 (1994); C. G. Van de Walle, *ibid.* **49**, 4579 (1994).

[36] Depassivation of a P_bH system can also be effectuated by providing an abundance of *atomic* H, i.e., the reverse of passivation reaction (1) (see, e.g., Refs. 7 and 23). This, however, involves different kinetics, leading only to partial dissociation.

[37] K. L. Brower, Phys. Rev. B **33**, 4471 (1986); A. Stesmans and J. Braet, in *Insulating Films on Semiconductors*, edited by J. J. Simone and J. Buxo (Elsevier, Amsterdam, 1986), p. 25.

[38] A. Stesmans and G. Van Gorp, Phys. Rev. B **42**, 3765 (1990); **45**, 4344 (1992).

[39] It may appear useful to add one more remark. In Brower's work (Ref. 18) on HP_b dissociation, *confined* to the range $T = 500-595\,^{\circ}\mathrm{C}$, depassivation data are plotted *relatively* as $[P_b]_{\mathrm{exp}}/[N_0]_{\mathrm{calc}}$ vs $[P_b]_{\mathrm{calc}}/[N_0]_{\mathrm{calc}}$, where $[N_0]_{\mathrm{calc}}$ represents the initial concentration of HP_b centers or the maximum concentration of recoverable P_b centers measured by ESR, as introduced in fitting the proposed theoretical $[P_b](T,t)$ expression (Eq. 4). No absolute values, either regarding $[P_b]$ or N_0, are plotted, with N_0 merely being left as a fitting parameter, albeit taken as constant. [However, it was mentioned (Ref. 18) that after thermal oxidation, $[P_b]$ is approximately $3\times10^{12}\,\mathrm{cm}^{-2}$.] In light of the data presented in Ref. 18, this is not incorrect: with the passivation temperature range being confined to below $\sim595\,^{\circ}\mathrm{C}$ (no additional creation of P_b sites), N_0 is *constant* (likely $\sim4.7\times10^{12}\,\mathrm{cm}^{-2}$) and this is only what matters.

[40] ''Nonexponential'' is used here to indicate that the $\log(1-[P_b]/N_0)$-vs-t curves are not straight lines [in contrast with the prescription of the ST model; Eq. (4)]. Clearly, Eq. (5) does not predict straight lines, although the behavior is fundamentally

exponential—not a simple one valued-E_d exponential decay, however.

[41] J. C. Nabity, M. Stavola, J. Lopata, W. C. Dautremont-Smith, C. W. Tu, and S. J. Pearton, Appl. Phys. Lett. **50**, 921 (1987).

[42] B. B. Stefanov, A. B. Gurevich, M. K. Weldon, K. Raghavachari, and Y. J. Chabal, Phys. Rev. Lett. **81**, 3908 (1998).

[43] This is not to be confused with another possible element of complication, namely, the possible disturbing impact of *atomic* H set free at the interface on the studied P_b-*molecular* hydrogen interaction kinetics.

[44] H. A. Kurtz and S. P. Karna (private communication).

[45] A. Borghesi, B. Pivac, A. Sassella and A. Stella, J. Appl. Phys. **77**, 4169 (1995).

[46] For reasons of completeness, we add that in a CV-probed study of interface trap *passivation* in forming gas (9% H_2; 91% N_2), Burte (Ref. 14) inferred the passivation process, rather than of nonexponential character, as described by a two-step process, each exhibiting simple exponential decay and characterized by activation energies of 0.18 ± 0.08 and 1.56 ± 0.11 eV, respectively. Based on a reported activation energy $E_a \sim 1.6$ eV for the diffusion of oxygen in SiO_2, the latter process was attributed to a reaction with oxygen, rather than passivation reaction (1).

[47] G. Schulze and M. Henzler, Surf. Sci. **124**, 336 (1983).

[48] P. Gupta, V. L. Calvin, and S. M. George, Phys. Rev. B **37**, 8234 (1988).

[49] K. L. Brower, P. M. Lenahan, and P. V. Dressendorfer, Appl. Phys. Lett. **41**, 251 (1982).

[50] A. G. Revesz, J. Electrochem. Soc. **126**, 122 (1979).

[51] J. Krauser, F. Wulf, M. A. Briere, J. Steiger, and D. Bräunig, Microelectron. Eng. **22**, 65 (1993).

[52] A. H. Edwards, J. A. Pickard, and R. E. Stahlbush, J. Non-Cryst. Solids **179**, 148 (1994).

[53] It is easily shown that for lower temperatures, i.e., high P_bH density, $[P_b\mathrm{H}]$ decays similarly in first- and second-order regimes, insofar as $k_d = k_d'$; the difference in the stretched out trend is most obvious at the higher-T end of the recovery region.